Proceedings of the Eleventh Asian Congress of Fluid Mechanics
22-25 May 2006, Kuala Lumpur, Malaysia

SURFACE SHEAR STRESS FLUCTUATIONS IN THE ATMOSPHERIC SURFACE LAYER

J. P. Monty [montyjp@unimelb.edu.au] and M. S. Chong
Department of Mechanical & Manufacturing Engineering University of Melbourne, Victoria, 3010 AUSTRALIA
N. Hutchins and I. Marusic
Department of Aerospace Engineering & Mechanics, University of Minnesota, Minneapolis, 55455 MN USA

ABSTRACT: A lightweight, high frequency response, floating element sensor was used to measure wall shear stress fluctuations in an atmospheric surface layer. The sensor uses a laser position measurement system to track the motion of the floating element. The measurements were taken as part of an internationally coordinated experimental program designed to make extensive spatial and temporal measurements of velocity, temperature and wall shear stress of the surface layer. Velocity measurements were made with both a $27m$ high vertical array and a $100m$ wide horizontal array of sonic anemometers; 18 anemometers in total were employed. Cross-correlations of shear stress and streamwise velocity fluctuations were analysed in an attempt to identify structure angles in the flow. The results were shown to compare favourably with experimental data from controlled, laboratory turbulent boundary layer measurements at three orders of magnitude lower Reynolds number.

1 INTRODUCTION

The measurement of wall shear stress is extremely important in the pursuit of a better understanding of the complex nature of turbulent boundary layers. This quantity is required for the determination of $U_\tau = \sqrt{\overline{\tau_w}/\rho}$, the friction velocity, from the mean wall shear stress, $\overline{\tau_w}$, and the fluid density, ρ. This velocity scale is almost universally employed in scaling arguments concerning turbulence statistics. It is not surprising, then, that the measurement of mean wall shear stress has received much attention in the literature[1]. In contrast, measurements of wall shear stress fluctuations, τ'_w, have received much less attention. This, however, is not an indication of the importance of such measurements. Fluctuating wall shear stress data are of interest to the Large Eddy Simulation (LES) community who currently rely on correlations with velocity to determine sub-grid scale τ'_w (this issue is addressed by Marusic *et al.*[2]). Furthermore, such measurements may reveal information about the physical structure of turbulence, and this is the topic of the following discussion.

The present work follows on from that of Heuer & Marusic[3] who developed a new, floating-element-type shear stress sensor. The device was designed primarily to measure τ'_w on the surface of the SLTEST site on the great salt lakes in Utah, USA. The unique facility that is the SLTEST site has been developed over a long period by Klewicki and coworkers[4, 5]. The geophysically driven, turbulent air flow over the site is thought to behave in a similar way to common wind-tunnel boundary layers, albeit at three orders of magnitude higher Reynolds number. While the extent of their similarities have not been conclusively established, elements of streamwise velocity and spectral scaling have been shown to compare favourably in both flows[6, 4]. Part of the motivation for this study was to further understand the similarities between the SLTEST surface layer and the wind tunnel boundary layer.

For comparison, Brown & Thomas[7] experimented with hot-film probes and hot-wire anemometers in a wind-tunnel-controlled, zero-pressure-gradient boundary layer. The boundary layer properties of relevance were: $Re_\theta = 10160$, $U_\tau = 1.280m/s$ and $\Delta = 0.040m$; where Re_θ is the Reynolds number based on momentum thickness and Δ is the 99% boundary layer thickness. Brown & Thomas[7] extensively analysed correlations between wall shear stress and streamwise velocity fluctuations. The velocity fluctuations were measured with an array of four hot-wire probes. It was conclusively shown by plotting peak correlation versus spatial separation, that, in the mean, structures of approximately 18° inclination dominate the flow. They interpret their results as evidence of characteristic hairpin eddies, similar to those assumed in the attached eddy model of Perry & Chong[8] and those observed in recent PIV studies[9, 10].

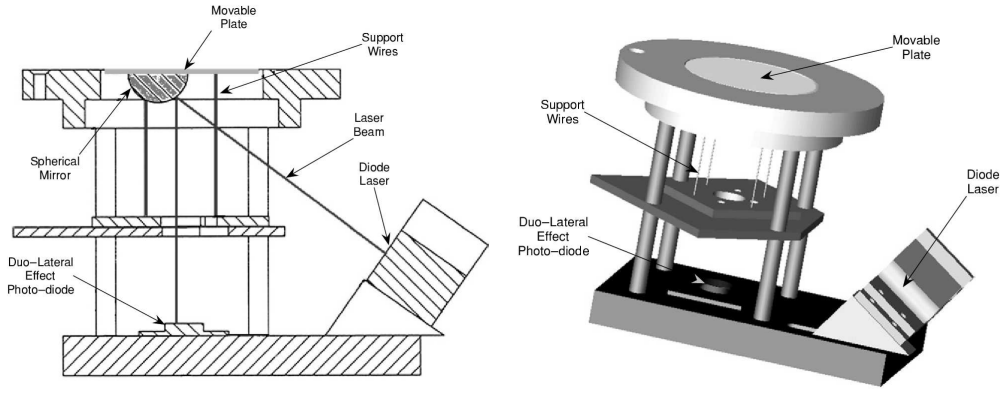

Figure 1: Schematic diagrams of the shear stress sensor (taken from Heuer & Marusic[3]).

2 EXPERIMENTAL APPARATUS

The surface layer at the SLTEST site is thought to have a thickness of approximately $\Delta = 100m$ as indicated from miniSODAR meaurements[4]. Common streamwise mean velocity magnitudes at the edge of the layer were in the vicinity of $10m/s$. Thus, an estimated Re_θ for the surface layer is $\mathcal{O}(10^6)$. This represents a flow of three orders of magnitude higher Re_θ than typical laboratory boundary layer flows, including, most pertinently, the study of Brown & Thomas[7]. At the time of experiment, the surface of the salt flats was extremely smooth as the surface had only recently dried out after long periods of heavy rain.

A $30m$ tower was erected with nine sonic anemometers, having logarithmic spacing, mounted on it. The lowest anemometer was mounted at $z = 1.42m$ from the surface, while the highest was mounted at $z = 25.69m$. The floating element shear stress sensor was placed directly below the sonic anemometer in the vertical array. The sensor was mounted flush with the surface by digging a pit below the sonic array and ensuring no significant steps or gaps between the edge of the pit and the sensor holder existed. All anemometers and the shear stress sensor were premanently oriented to face north.

The floating element shear stress sensor was essentially the same as that constructed by Heuer & Marusic[3] and is shown in figure 1. The present authors inserted a UV filter over the photo-diode to reduce the effects of sunlight, and the diode laser mount was modified in an attempt to reduce sensor drift due to thermal expansion of the original mount[1]. Preliminary tests confirmed the latter modification was successful, although drift was not fully removed; the UV filter made moderate improvement, however, day-time results will not be discussed and so this modification is irrelevant for the purposes of this paper. Calibration of the sensor was carried out in an identical manner to that discussed in Heuer & Marusic[3].

All signals were sampled using a Campbell Scientific weatherproof data acquistion system. Sonic anemometer and shear stress sensor outputs were sampled at $20Hz$ continuously throughout each day for approximately seven days. This sampling frequency was considered adequate given that the smallest eddies of interest had characteristic frequencies of $\mathcal{O}(1)Hz$. Fortunately, sufficiently strong northerly winds prevailed continuously for a number of days after the data acquisition system was initialised. However, five days into the experiment, severe weather — bringing frequent southerly winds — rendered days 6 and 7 data meaningless. Futhermore, the shear stress sensor was permanently deactivated in the accompanying rainstorm on day 7. Despite this setback, five days of almost unwavering north wind gave more than enough sampling time for the analysis presented here.

3 RESULTS

All analyses presented in this section involved only a fraction of the amassed data for the sake of brevity. The representative data set chosen for presentation contained 66 minutes of continuous data sampled during the night. Somewhat surprisingly, the heat flux, $\overline{u_3\theta'}$, over the measured surface layer remained

[1]These modifications are not included in the schematic diagrams of figure 1.

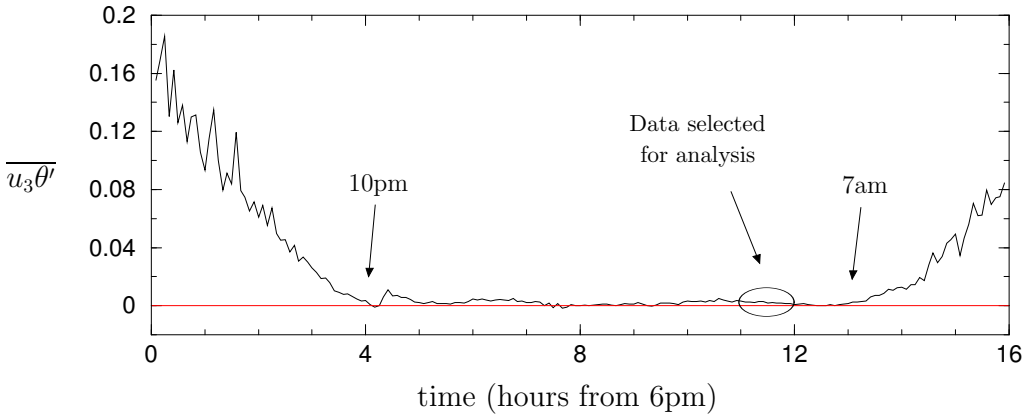

Figure 2: Typical 5 minute averages of $\overline{u_3\theta'}$ during the evening, through the night and into the morning. The data set selected for analysis is circled. This data is referred to in the text as the 'chosen data'.

constant and very near zero throughout the night; figure 2 illustrates this point. Also shown in the figure is the time window of data selected for more detailed analyses to follow in this paper. Clearly, the selected data is in a region of very low heat flux. We will refer to data from this time frame as the 'chosen data'. For an atmospheric surface layer to be compared to laboratory-type boundary layers (where heat flux is zero), the layer is required to be *neutral*. That is, the energy production due to turbulent shear overwhelms that due to buoyancy factors[11]. The neutrality of a surface layer may be determined by the Monin-Obukhov length, L, defined as

$$L = -\frac{\Theta U_\tau^3}{g\kappa\overline{u_3\theta'}}, \tag{1}$$

where Θ is the mean temperature, $g = 9.81ms^{-2}$ is the gravitational acceleration, and $\kappa = 0.395$ is the log law constant. A surface layer is said to become neutral as $1/L \to 0$. For the chosen data set, $1/L = -2.336 \times 10^{-3}m^{-1}$, indicating that the layer should be considered neutral during this time (in fact, this indicates that buoyancy forces do not become as significant as turbulent shear forces until a height of $z = -0.5L \approx 214m$). It must be noted that the chosen data set does not have especially unique properties. Many data sets were analysed at various times through the night with strikingly similar results for all of the five 24-hour periods of data available.

Firstly, a typical mean velocity profile, calculated from the chosen data, is shown in figure 3 with near-wall scaling. The friction velocity was found using the Clauser[12] method[2]. Log law constants of $\kappa = 0.395$ and $A = 4.6$ were employed for this method. It was found that $U_\tau = 0.234m/s$ determined as such resulted in a value approximately 8% higher than that determined from assuming the *scaled* Reynolds shear stress is constant and approximately unity, i.e., $U_\tau^2 = -\overline{u_1u_3}$. Nevertheless, such uncertainty in U_τ will not alter the conclusions of this study.

Second order turbulence statistics for the chosen data are also presented in figure 3. Since only one Reynolds number has been considered here, the statistics may be shown with both inner and outer flow scaling. The trends of the statistics are typical of night-time measurements taken at the SLTEST site. Perhaps of most importance in this plot is the constancy of Reynolds shear stress throughout the measured portion of the layer. This constancy was consistently observed in many data sets and was required for the calculation of friction velocity via $U_\tau^2 = -\overline{u_1u_3}$. Friction velocity calculated in this way was used to relate the mean surface shear stress and the mean voltage of the shear stress sensor.

One of the main objectives of this study was to determine whether characteristic structure angles in the

[2]Since sunlight and sensor drift problems were not certainly eliminated, the shear stress sensor mean voltage was not used to determine $\overline{\tau_w}$.

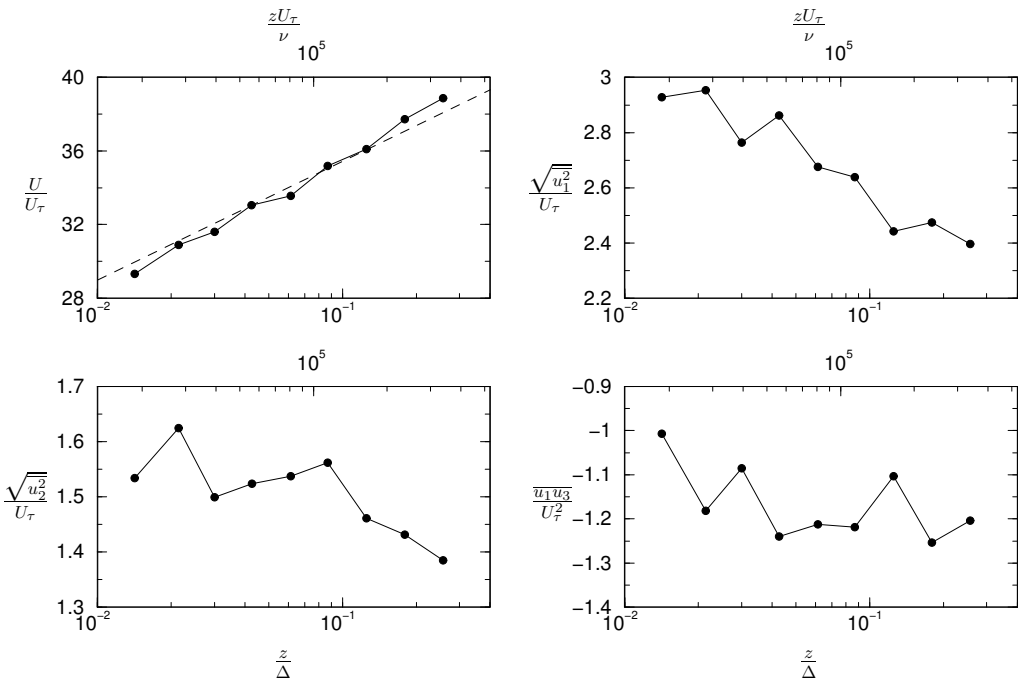

Figure 3: Turbulence statistics calculated from the chosen data set. In the mean velocity plot (top-left) the broken line represents a log law with constants $\kappa = 0.39$ and $A = 4.6$.

flow could be found and, further, whether such structures behaved in a similar way to those in a laboratory boundary layer. For comparison, a laboratory turbulent boundary layer study that includes measurement of wall shear stress fluctuations, τ'_w, is required. One such study is that documented in Brown & Thomas[7], as described in the introduction. At this point, the reader will recall that Brown & Thomas showed a strong trend of structures making angles of roughly 18° with the mean flow direction. Furthermore, a previous study at the SLTEST site[3], reported a mean structure angle of 14.2°. In that study, only one z-level streamwise velocity time-series was available for correlation with the wall shear stress, and that was at $z = 0.24m = 0.0024\Delta$ — significantly lower than the lowest sonic anemometer of the present work.

The sonic anemometer array at the SLTEST site provided a convenient, continuous time-series of velocity data, as discussed earlier. Streamwise wall shear stress fluctuations measured with the floating element sensor were correlated with u_1 measurements from each sonic, giving a total of 9 correlation plots. Figure 4 displays two of these correlation distributions. As expected, the peaks of the correlations do not coincide and are both displaced from $x = 0$ — the streamwise location of the sonic anemometers. The inset plot, which is simply a closer view of the correlation peaks, clearly illustrates these features. Note that Taylor's frozen turbulence hypothesis was employed to convert from the temporal to the spatial domain and the convection velocity used was the local mean streamwise velocity.

All nine z-level correlations are plotted as a contour plot in figure 5. This figure allows a clear identification of correlated structure angle. It should be noted that the correlation distributions were normalised with their peak magnitudes for this figure. Perhaps the most striking feature of this plot is the strong ridge of peak correlation (dark red) extending to the top of the anemometer array ($z = 0.2569\Delta$). This ridge suggests that the flow is made up of very well-defined cohesive structures — even at $25.69m$ above the surface.

The dark solid lines plotted over the contours are shown to aid the inference of structure angle, γ, from the contours. It appears that an angle of $\gamma \approx 15^\circ$ is a reasonable estimate, which is in excellent agreement with the study of Brown & Thomas[7] and Heuer & Marusic[3]. In his paper on vortex packets, Marusic[13] uses packets of attached hairpin eddies in the Perry & Chong attached eddy model (see figure

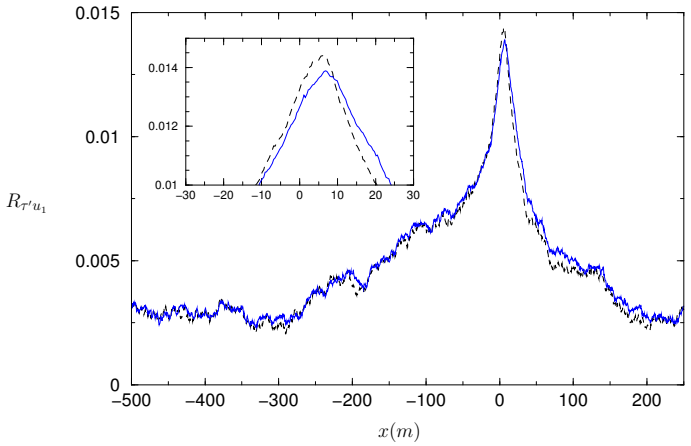

Figure 4: Correlations of wall shear stress and velocity fluctuations at two z-levels. The broken line corresponds to $z = 1.42m = 0.0142\Delta$, while the solid line corresponds to $z = 2.14m = 0.0214\Delta$.

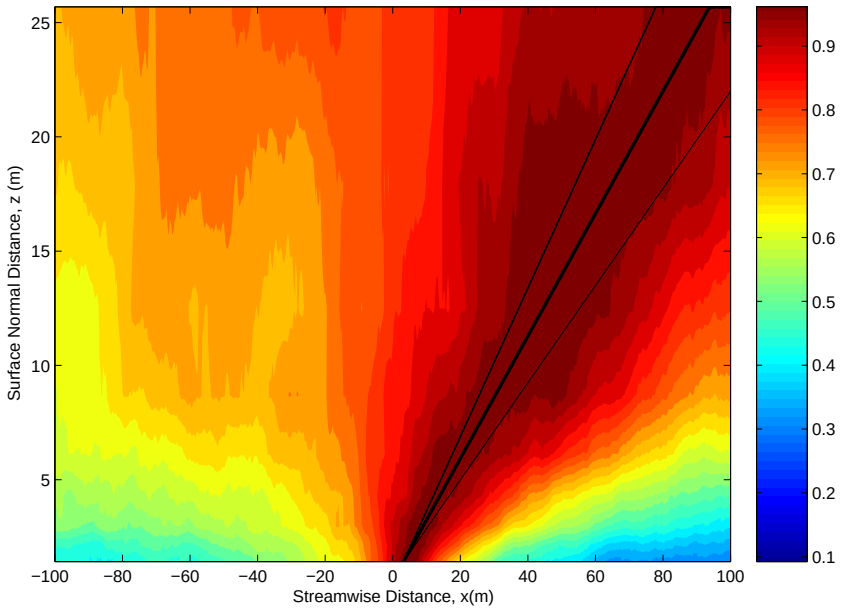

Figure 5: Contour plot of correlations of wall shear stress and velocity fluctuations at all z-levels. Solid lines are simply straight lines making angles of 12°, 15° (heavy line) and 18° with the x-direction.

6 for illustration of eddy packets). The 'heads' of these hairpins were inclined at approximately $15.5°$ and the model results displayed excellent agreement with experiment. Yet more evidence may be found in the investigation of Ganapathasubramani *et al.*[14], which suggests $\gamma = 12$–$13°$. This value is also not significantly dissimilar to the result presented here.

Brown & Thomas present a possible interpretation of the angle γ: the angle of inclination of a single hairpin-type attached eddy. Since their study in 1977, there has been considerable evidence suggesting characteristic single hairpin eddies have angles closer to $45°$[9, 14, 13]. In light of this and other recent findings concerning hairpin vortices in turbulent shear flows, a better interpretation of γ may be the angle of hairpin

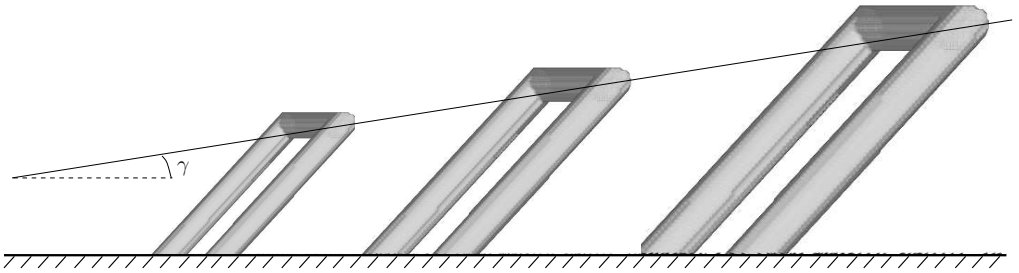

Figure 6: An illustration of three attached hairpin eddies forming part of a coherent 'packet' and having a head inclination angle γ.

'heads' in a packet of attached eddies. This interpretation is illustrated in figure 6.

Finally, it should be noted that the use of the Taylor hypothesis must have an affect on the inferred structure angle. However, it was found through trials of various convection velocities that variations in γ did not exceed 3°. Therefore, the authors are confident that the Taylor hypothesis has not affected the conclusions of this study.

4 CONCLUSIONS

Measurements of various turbulence statistics throughout the surface layer at the SLTEST site show indications of laboratory-boundary-layer-like behaviour. Most pertinently to this investigation, analyses of shear stress-velocity correlations show strong signs of coherent, characteristic structures making angles of roughly 15° to the wall. This angle could be interpreted as the characteristic inclination of hairpin heads in a packet of attached eddies. Although there were known problems with the shear stress sensor employed (e.g. UV light sensitivity, unreliable mean measurement), these appear to have had, at worst, a small impact on the results presented. Comparisons with controlled, boundary layer measurements (having almost three orders of magnitude lower Re) indicate that similar structure angles exist in both flows. This is encouraging from the point of view that typical laboratory measurements may have significant relevance to real-world, uncontrolled flows at much higher Reynolds number.

REFERENCES

[1] Naughton JW and Sheplak M: Modern developments in shear-stress measurement. *Prog. in Aero. Sci.*, 2002. **38**, 515–570.

[2] Marusic I, Kunkel GJ and Porté-Agel F: Experimental study of wall boundary conditions for large-eddy simulation. *J. Fluid Mech.*, 2001. **446**, 309–320.

[3] Heuer WDC and Marusic I: Turbulence wall-shear stress sensor for the atmospheric surface layer. *Meas. Sci. Tech.*, 2005. **16**, 1644–1649.

[4] Metzger MM and Klewicki JC: A comparative study of near-wall turbulence in high and low Reynolds number boundary layers. *Phys. Fluids*, 2001. **13**, 692–701.

[5] Klewicki JC, Foss JF and Wallace JM: High Reynolds number $[\mathrm{Re} = \mathcal{O}(10)^6]$ boundary layer turbulence in the atmospheric surface layer above western utah's salt flats. In RJ Donnelly and KR Sreenivasan, editors, *Flow at Ultra-High Reynolds and Rayleigh numbers*. 450–466.

[6] Kunkel GJ and Marusic I: Study of the near-wall turbulent region of the high-reynolds-number boundary layer using an atmopheric flow. *J. Fluid Mech.*, 2005.

[7] Brown GL and Thomas ASW: Large structure in a turbulent boundary layer. *Phys. Fluids*, 1977. **20**(10), S243–252.

[8] Perry AE and Chong MS: On the mechanism of wall turbulence. *J. Fluid Mech.*, 1982. **119**, 173–217.

[9] Adrian RJ, Meinhart CD and Tomkins CD: Vortex organization in the outer region of the turbulent boundary layer. *J. Fluid Mech.*, 2000. **422**, 1–54.

[10] Ganapathisubramani B, Longmire EK and Marusic I: Characteristics of vortex packets in turbulent boundary layers. *J. Fluid Mech.*, 2003. **478**, 35–46.

[11] Stull RB: *An introduction to boundary layer meteorology*. Dordrecht: Kluwer, 1997.

[12] Clauser FH: Turbulent boundary layers in adverse pressure gradients. *J. Aero. Sci.*, 1954. **21**, 91–108.

[13] Marusic I: On the role of large-scale structures in wall turbulence. *Phys. Fluids*, 2001. **13**, 735–743.

[14] Ganapathisubramani BB, Hutchins N, Hambleton WT, Longmire EK and Marusic I: Large-scale coherence in a turbulent boundary layer. *J. Fluid Mech.*, 2005. **524**, 57–80.